Transcriptomic network analyses shed light on the regulation of cuticle development in maize leaves

Pengfei Qiao[a], Richard Bourgault[b], Marc Mohammadi[b], Susanne Matschi[c], Glenn Philippe[a], Laurie G. Smith[c], Michael A. Gore[d], Isabel Molina[b,1], and Michael J. Scanlon[a,1]

[a]Plant Biology Section, School of Integrative Plant Science, Cornell University, Ithaca, NY 14853; [b]Department of Biology, Essar Convergence Centre, Algoma University, Sault Ste. Marie, ON P6A 2G4, Canada; [c]Section of Cell and Developmental Biology, University of California San Diego, La Jolla, CA 92093; and [d]Plant Breeding and Genetics Section, School of Integrative Plant Science, Cornell University, Ithaca, NY 14853

Edited by Dominique C. Bergmann, Stanford University, Stanford, CA, and approved April 9, 2020 (received for review March 16, 2020)

Plant cuticles are composed of wax and cutin and evolved in the land plants as a hydrophobic boundary that reduces water loss from the plant epidermis. The expanding maize adult leaf displays a dynamic, proximodistal gradient of cuticle development, from the leaf base to the tip. Laser microdissection RNA Sequencing (LM-RNAseq) was performed along this proximodistal gradient, and complementary network analyses identified potential regulators of cuticle biosynthesis and deposition. A weighted gene coexpression network (WGCN) analysis suggested a previously undescribed function for PHYTOCHROME-mediated light signaling during the regulation of cuticular wax deposition. Genetic analyses reveal that *phyB1 phyB2* double mutants of maize exhibit abnormal cuticle composition, supporting the predictions of our coexpression analysis. Reverse genetic analyses also show that *phy* mutants of the moss *Physcomitrella patens* exhibit abnormal cuticle composition, suggesting an ancestral role for PHYTOCHROME-mediated, light-stimulated regulation of cuticle development during plant evolution.

cuticle | maize | PHYTOCHROME- | network | evolution

Light signaling plays an important role in the regulation of plant metabolism and development (1–4), including the activation of genes involved in biosynthesis of the cuticle (5–7). Cuticles form the hydrophobic barrier deposited on the epidermis of all land plants, which restricts nonstomatal water loss and enabled plants to colonize the terrestrial environment. Since the majority of water loss in plants occurs through the epidermis, the cuticle imparted a significant advantage during land plant evolution by providing a barrier to desiccation (8–12).

Plant cuticles comprise mixtures of solvent-soluble lipids (waxes) and lipid polymers (cutin), although their precise structure and composition vary greatly among plant species, cells/tissues/organs, and developmental stages (13, 14). Waxes are long-chain, nonpolar molecules, composed mainly of hydrocarbons (alkanes and alkenes), aldehydes, alcohols, ketones, and wax esters. In contrast, cutins are polymers of hydroxy fatty acids connected by ester bonds (14–17). Waxes and cutins are both formed de novo from long-chain (C_{16} and C_{18}) fatty acids synthesized within plastids of the plant epidermis (17–21). In *Arabidopsis thaliana*, these long-chain fatty acids are converted to Coenzyme A (CoA) thioesters by LONG-CHAIN ACYL-COA SYNTHASE and subsequently transported into the endoplasmic reticulum, where they are elongated by the fatty acid elongase complex to produce wax precursors (5). After modification of very-long-chain and long-chain acyl-CoAs to form wax components and cutin monomers, respectively, these cuticle lipids are exported across the plasma membrane and into the apoplastic space, the site of cuticle deposition. Cutin monomers are further polymerized at the cell wall surface by an extracellular "polyester synthase" of the Glycine-Aspartic acid-Serine-Leucine–motif family (17, 22). Cuticle biosynthesis is regulated by developmental and environmental factors such as the phytohormone abscisic acid, water deficit, osmotic stress, and light (5–7). Furthermore, cuticle biogenesis is subjected to transcriptional, posttranscriptional, and posttranslational controls (23).

Previous studies of maize cuticles have focused on juvenile leaves and the glossy mutants, which together define >30 loci required for normal deposition of epicuticular waxes on the leaf surface (24). Eight glossy genes have been cloned, most of which encode homologs of genes known to function during cuticle biosynthesis or its transcriptional regulation. The genetic basis of cuticle formation and function in adult maize leaves, where cuticle properties are expected to have the biggest impact on drought tolerance and other agronomically important traits, is largely unexplored (25).

In this study, we utilized the expanding adult leaf as a model system to elucidate the spatial–temporal gradient of maize cuticle development. Transcriptomic analyses were performed along the proximodistal axis of the developing maize leaf 8, as it emerged from darkness to light. A weighted gene coexpression network (WGCN) analysis was used to identify patterns of epidermal gene expression underlying the previously identified, proximodistal cuticle-composition gradient within the expanding adult leaf (25) and to identify both predicted and previously undescribed candidate genes for cuticle development in maize. Notably, our network analyses suggested a previously undescribed role for PHYTOCHROME light receptors during the regulation of cuticle development, which is supported by genetic and biochemical investigations in the evolutionarily divergent model plants *Zea mays* and *Physcomitrella patens*. We propose a model whereby

Significance

Plant cuticles provide barriers to water loss and arose as aquatic plants adapted to the dry terrestrial environment. The cuticle components, waxes and the fatty acid-based polymer cutin, are synthesized in the plant epidermis, exported across the cell wall, and deposited on the plant surface. This study suggests a role for PHYTOCHROME light receptors during cuticle development in leaves of maize and moss, diverse species that are separated by more than 400 million y of land plant evolution. We hypothesize that phytochrome-mediated light signaling contributed to the evolution of cuticles in land plants.

Author contributions: P.Q., L.G.S., M.A.G., I.M., and M.J.S. designed research; P.Q., R.B., M.M., S.M., and G.P. performed research; P.Q., R.B., I.M., and M.J.S. analyzed data; and P.Q., I.M., and M.J.S. wrote the paper with input from L.G.S. and M.A.G.

The authors declare no competing interest.

This article is a PNAS Direct Submission.

Data deposition: The raw RNAseq data are available at NSBI Short Reads Archive (SRA; accession no. SRP116320).

[1]To whom correspondence may be addressed. Email: isabel.molina@algomau.ca or mjs298@cornell.edu.

This article contains supporting information online at https://www.pnas.org/lookup/suppl/doi:10.1073/pnas.2004945117/-/DCSupplemental.

First published May 18, 2020.

phytochrome-mediated light signaling was a critical step contributing to the evolution of cuticle development in the land plants.

Results and Discussion

Transcriptomic Analyses of Cuticle Development in the Adult Maize Leaf. Previous analyses demonstrated a gradient of cuticle maturation along the proximodistal axis of the expanding leaf 8 of maize inbred line B73, from light-shielded proximal intervals (0 to 16 cm from the leaf base) to light-exposed distal regions (Fig. 1*A*). In general, longer-chain wax components and cutin monomers increase in abundance as the leaf transitions from the dark to light (25). To capture the transcriptional gradient coinciding with these biochemical changes in cuticle composition, plants were grown under the same conditions as in Bourgault et al. (25), and seven developmental stages along the proximodistal axis of leaf 8, representing the full spectrum of cuticle maturation stages, were laser microdissected for RNA sequencing (RNAseq) analysis (Fig. 1*B*). Each stage comprised a 2-cm-long interval, collected between 2 and 22 cm from the leaf base, which included the point of emergence of leaf tissue into the light at ~17 to 18 cm (Fig. 1*A*). For each of the seven proximodistal intervals examined, an L1-derived epidermal sample and an L2-derived internal sample were laser microdissected (Fig. 1*B*) followed by RNAseq to construct their respective transcriptomes.

Principal component analysis (PCA) identified two principal components (PCs) that collectively explain 60.29% of the total sample variance in the transcriptomic data. Specifically, the first PC corresponds to the seven proximodistal leaf intervals analyzed and explains 38.22% of the total sample variation, whereas the second PC (PC2; 22.07% of sample variance) delineates epidermal and internal tissues for each leaf developmental stage (Fig. 1*C*). These data show that in addition to a biochemical gradient in cuticle composition, the leaf intervals examined in the expanding maize leaf 8 also exhibit a transcriptomic gradient.

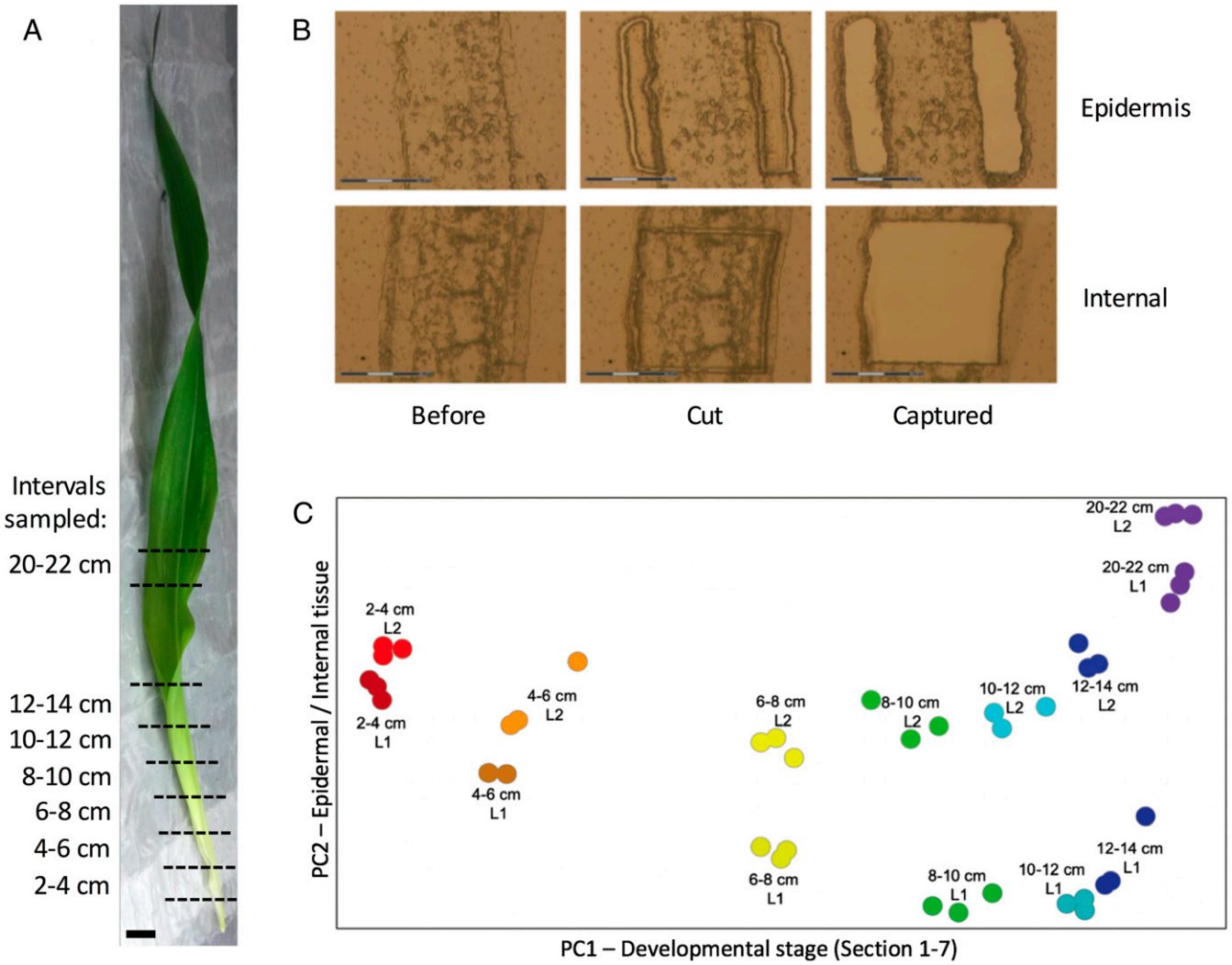

Fig. 1. Transcriptomic analyses along the proximal–distal axis of the maize adult leaf. (*A*) Expanding maize leaf 8. Dashed lines demarcate the boundaries of 2-cm intervals collected along the proximodistal axis (note: the leaf emerges from the whorl into the light ~18 cm from the leaf base). (Scale bar: solid line, 2 cm.) (*B*) Laser microdissection was performed on leaf tissues to isolate the L1-derived epidermal layers (*Upper*) and L2-derived internal layers of each targeted leaf interval (*A*) along the proximodistal axis of the expanding leaf 8. From left to right, each column corresponds to a leaf section (*Left*) before microdissection, (*Center*) after isolation of the target tissue from surrounding tissue, and (*Right*) after laser microdissection. (Scale bars: 75 μm.) (*C*) PCA identified two PCs corresponding to the developmental stage (PC1) and tissue type (PC2) of leaf 8 samples in our LM-RNAseq analysis. Each point corresponds to one RNAseq sample. From left to right, each color corresponds to a specific developmental stage (youngest to oldest part of the leaf). From bottom to top, darker color shades represent L1-derived epidermal tissues (L1), and lighter shades represent L2-derived (L2) internal tissues. For interval 2, one outlier epidermal sample was removed.

A Weighted Coexpression Network Analysis Identifies Candidate Regulatory Genes for Cuticle Biosynthesis. Genes differentially expressed in the epidermis (where cuticle biogenesis occurs) during different stages along the cuticle maturation gradient were queried for relationships to known cuticle biosynthesis genes identified previously in *A. thaliana* (Dataset S1). In most cases, maize presented two or more duplicate loci with high homology to individual Arabidopsis cuticle genes. Detailed summaries of the pathways for plant cuticle biosynthesis and in-depth transcript accumulation patterns of predicted maize candidate genes expressed during leaf 8 cuticle maturation are provided in *SI Appendix*, Fig. S1 and Dataset S1. We next used a gene coexpression network (GCN) analysis (26, 27) to identify additional candidate genes involved in regulating the biosynthesis of the maize cuticle. A GCN is essentially a "guilt-by-association" approach, wherein correlations in gene expression levels implicate coregulation of transcript pairs (nodes) within the network. In a WGCN, each edge (correlation between gene expression levels) is calculated to indicate the strength of its coexpression relationship with every other node in the network (26). In this way, a WGCN was constructed based upon the expression-level correlations of all 11,816 epidermally transcribed genes identified in our laser microdissection RNA Sequencing (LM-RNAseq) analysis.

Our WGCN partitioned the transcriptome of the emerging leaf 8 into 21 coexpression modules (Datasets S2–S22). Fig. 2 illustrates the expression levels of eigengenes (idealized representative genes) within these 21 modules at each of the seven leaf developmental stages analyzed. Major developmental trends are shown in Fig. 2. Expression levels of genes within modules F to I are positively correlated with the accumulation of wax esters, cutin, and alkanes with chain lengths longer than 29 carbons. In contrast, transcripts comprising modules L to O display decreasing levels of accumulation from the proximal to distal intervals of the leaf, similar to the pattern of $C_{21:0}$ to $C_{29:0}$ hydrocarbon accumulation in the expanding leaf cuticle (Fig. 2). Thus, comparisons of transcript accumulation levels with cuticle lipid profiles at each proximodistal leaf interval (Fig. 2) reveal interesting correlations, clearly identifying a set of "immature" cuticle coexpression modules (L to O) and "mature" cuticle modules (F to I). Many modules that are positively or negatively correlated with specific

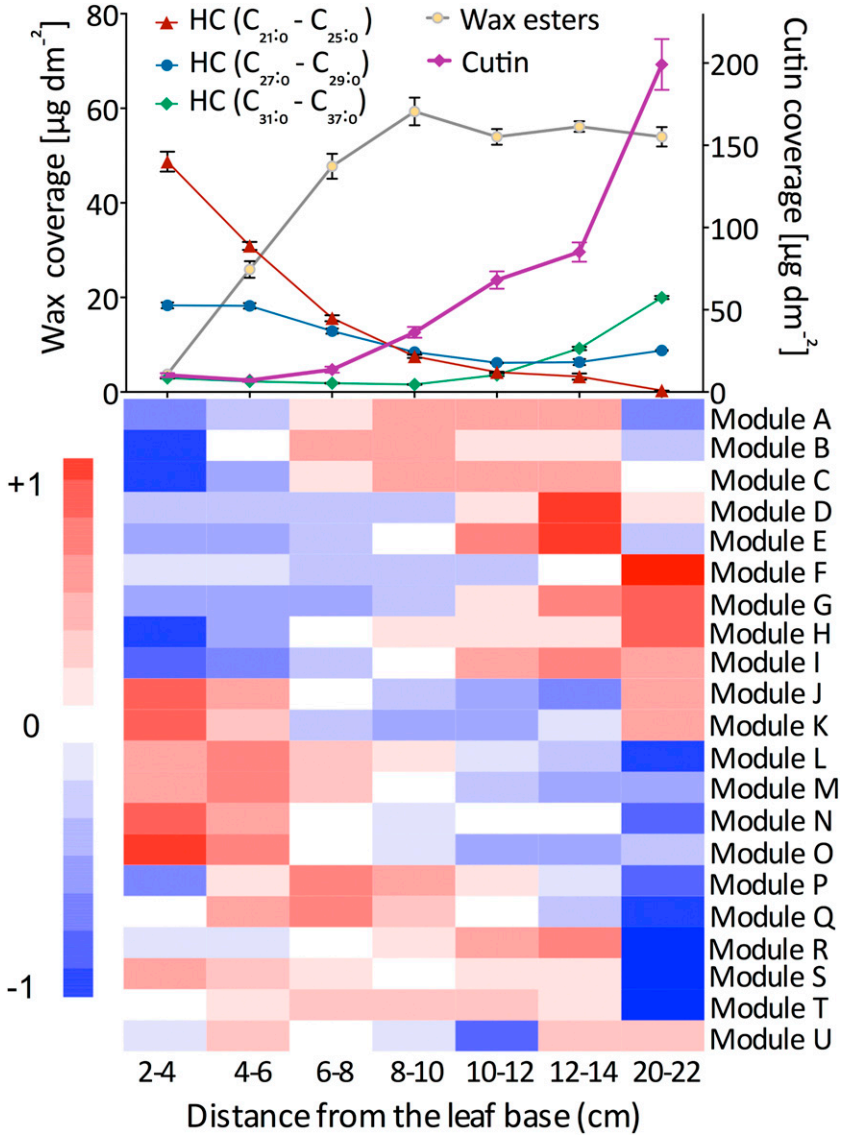

Fig. 2. Proximodistal transcriptomic gradients in the expanding adult maize leaf. Changes in the accumulation of the most predominant cuticle components, namely cutin, wax esters, and hydrocarbons (HC), are compared with the expression levels of eigengenes for the 21 modules identified in our WGCN analysis. (*Upper*) Reproduced from ref. 25, which is licensed under CC BY 4.0.

cuticle lipid profiles contain transcripts from known cuticle biosynthesis and regulatory genes (Dataset S1). Within module F, for example, the KCS6/CER6 homologs AC233893.1_FG003 and GRMZM2G060481 show correlation coefficients of 0.95 and 0.81 with 35:0 alkane, whereas the KCS1 homolog GRMZM2G104626, found in module H, has a correlation coefficient >0.90 with alkanes 31:0 to 35:0. The strategic use of this WGCN network analysis for gene discovery is described below.

One such strategy was to interrogate the "direct neighbors" of known cuticle biosynthetic genes within the network, as demonstrated in analyses of six modules (A, C, F, H, I, and Q) showing enrichment for known cuticle gene transcripts. For instance, transcripts from several gene families known to function in cuticle biosynthesis are overrepresented in module F, including *KCS*s, *ABC TRANSPORTER*s, and *LTP*s, whose direct neighbors exhibit strong coexpression with these cuticle candidate genes, thereby implicating regulatory or coregulatory roles. Direct neighbors of known cuticle biosynthesis gene transcripts within these modules are summarized in Dataset S23 and comprise potential candidate genes involved in the regulation of cell wall modifications—including cuticle biosynthesis—in the expanding adult maize leaf (27, 28). Furthermore, epidermally enriched transcripts are overrepresented in these coexpression modules. For example, out of 972 gene transcripts within module F, 41.26% are up-regulated in the epidermis, whereas only 31.89% of all of the 11,816 epidermally transcribed genes are up-regulated in the epidermis. This additional layer of spatial filtering further supports an association between these coexpression modules and cuticle biogenesis.

A second gene discovery approach enabled by WGCN analyses is to examine the hubs within the network, defined as the most connected nodes that are essential to network function (29, 30). In our case, the hubs of coexpression modules that are significantly correlated with cuticle components are usually a subset of the candidates identified via the direct neighbor approach described above. For example, in module F many of the hubs are also direct neighbors of gene transcripts from *KCS*s, *ABC TRANSPORTER*s, and *LTP*s. Two of these hubs are among the DE up-regulated genes in the epidermis. These data further support the importance of module F, and especially its hubs, during cuticle development in the expanding adult maize leaf. In fact, 11% of the epidermally up-regulated candidates for cuticle biosynthesis/regulation are found in module F (Dataset S1). Other modules in Dataset S1 that are enriched for epidermally up-regulated candidates include modules O (14% of epidermally enriched candidates), H (12%), A (10%), C (7%), L (9%), Q (6%), and T (6%). Four additional hub genes within modules A, C, and Q are also included in the cuticle candidate gene list. However, many additional hubs that are not initially identified as containing cuticle candidate genes following homolog annotation are highlighted in our WGCN analysis, providing potentially novel candidate genes correlate with cuticle components (Dataset S23).

Light-Regulated Cuticle Development: *Phytochrome* (*phy*) Mutants Have Altered Cuticle Composition. Previous studies showed that light induces cuticular wax biosynthesis in land plants, and the expression levels of several fatty acid elongase complex transcripts decrease in dark-grown plants, thus reducing the amount of cuticular wax (1, 4–7, 31). Moreover, biochemical analyses also revealed that longer-chain wax components are more abundant in the distal, light-exposed intervals of maize leaf 8 (Fig. 2) (25). Interestingly, although algal relatives of the land plants do not develop a cuticle, light exposure induces the conversion of hydrocarbons from long-chain fatty acids in algae (32, 33). A Gene Ontology term analysis of coexpression module H (another of the six modules enriched in cuticle genes) showed significant enrichment for light-responsive transcripts, including five *PHYTOCHROMES* (*PHY*s; *PHYA1*, *PHYA2*, *PHYB1*, *PHYC1*, and *PHYC2*) (Fig. 3*A* and *SI Appendix*, Fig. S2). PHYTOCHROMES are red/far-red light photoreversible chromoproteins that regulate gene expression in response to light. Maize contains six PHY homologs (PHYA1, PHYA2, PHYB1, PHYB2, PHYC1, PHYC2) (34). Our WGCN identified the photoreceptors *PHYB1* and *PHYA1* as major hubs in module H (Fig. 3*A*), whereas *PHYA2* and *PHYC1* contain far fewer edges. We note that *PHYB2* transcripts are identified in internal tissue layers but not the epidermis of the emerging maize leaf 8; thus, *PHYB2* does not appear in module H. Intriguingly, previous studies in *Arabidopsis* revealed noncell-autonomous PHYB function throughout plant development, including during the regulation of flowering time, stomatal development, and hypocotyl gravitropism (35–37). Accumulation of *PHYB1*, *PHYA1*, and *PHYA2* transcripts, and module H in general, is negatively correlated with hydrocarbon compounds (alkenes and $<C_{31}$ alkanes) that are found in the immature cuticle, which is embedded within the whorl and shielded from light (Fig. 3 *B* and *C*). Conversely, the module H eigengene, as well as the transcript accumulation of *PHYB1*, *PHYA1*, and *PHYA2*, positively correlates with mature cuticle components, such as alkanes > C_{31}, wax esters, and cutin monomers (Fig. 3 *B* and *C*).

To investigate possible functions for phytochromes in cuticle biogenesis, we next conducted chemical analysis of cuticle components in the first adult-staged leaf of previously described maize *phy* mutants (described in *Plant Materials*) (38, 39). Specifically, three predicted null alleles of *phyb1*, two allele combinations of *phyb1 phyb2* double mutants, and a *phya1 phya2* double mutant were analyzed in the maize inbred W22 background, wherein leaf 9 comprises the first adult leaf. No significant changes in leaf 9 cuticle components were consistently identified in the *phyb1* single-mutant alleles. Although previous analyses revealed some subfunctionalization of the PHYB paralogs in maize, a wide range of PHYB1 and PHYB2 seedling and mature plant functions are genetically redundant (38). As such, both allelic combinations of *phyb1 phyb2* double mutants (i.e., *phyb1- phyb2-1* and *phyb1-phyb2-2*) showed increased levels of total alkanes and total free fatty acids in leaf 9 cuticles as compared with wild-type W22 controls (Fig. 4*A*). Specifically, C_{16}, C_{18}, and C_{36} fatty acids are overabundant in both *phyb1 phyb2* double-mutant cuticles. Perhaps more strikingly, the alkane classes C_{23}, C_{25}, C_{27}, C_{29}, and C_{37} are all significantly increased in *phb1 phyb2* mutants (Fig. 4*B*). Only one of the double-mutant combinations however, *phb1 phyb2-2*, showed significant increases in the accumulation of fatty alcohols and aldehyde classes (increased levels of C_{24} to C_{32} and C_{26} to C_{30} species, respectively) (*SI Appendix*, Fig. S3), although the *phyb1 phyb2-1* allele did show similar trends (Fig. 4*B*). These results validate the predictive power of our WGCN data and suggest that PHYB-mediated light signaling may function to repress the accumulation of specific cuticle components in light-exposed regions of the maize adult leaf. Interestingly, the defects in alkane cuticle composition observed in the *phyb1 phyb2* double mutants mirror the changes in alkane components of the cuticle as the leaf emerges from the whorl (Fig. 2) (25). Namely, a shift from shorter to longer hydrocarbons ensues after exposure to light, wherein chain lengths of <30 carbons predominate in dark-exposed leaf intervals. Further support for this model of PHYB-mediated regulation of cuticle composition is provided by the positive correlations between *PHYB1* transcript accumulation and hydrocarbons with chain lengths of >31 carbons and a corresponding negative correlation with shorter ones (<31 carbons) (Figs. 2 and 3 *B* and *C*).

The two maize *PHYA* paralogs show largely overlapping patterns and levels of transcript accumulation, which suggest highly redundant functions (34, 39). Intriguingly, although only a single allele combination of the *phya1 phya2* double mutant is available and no morphological or developmental phenotypes have been described previously for *phya* single or double mutants (39), gas chromatography–mass spectrometry analyses revealed significant overaccumulation of total wax esters in *phya1 phya2* double

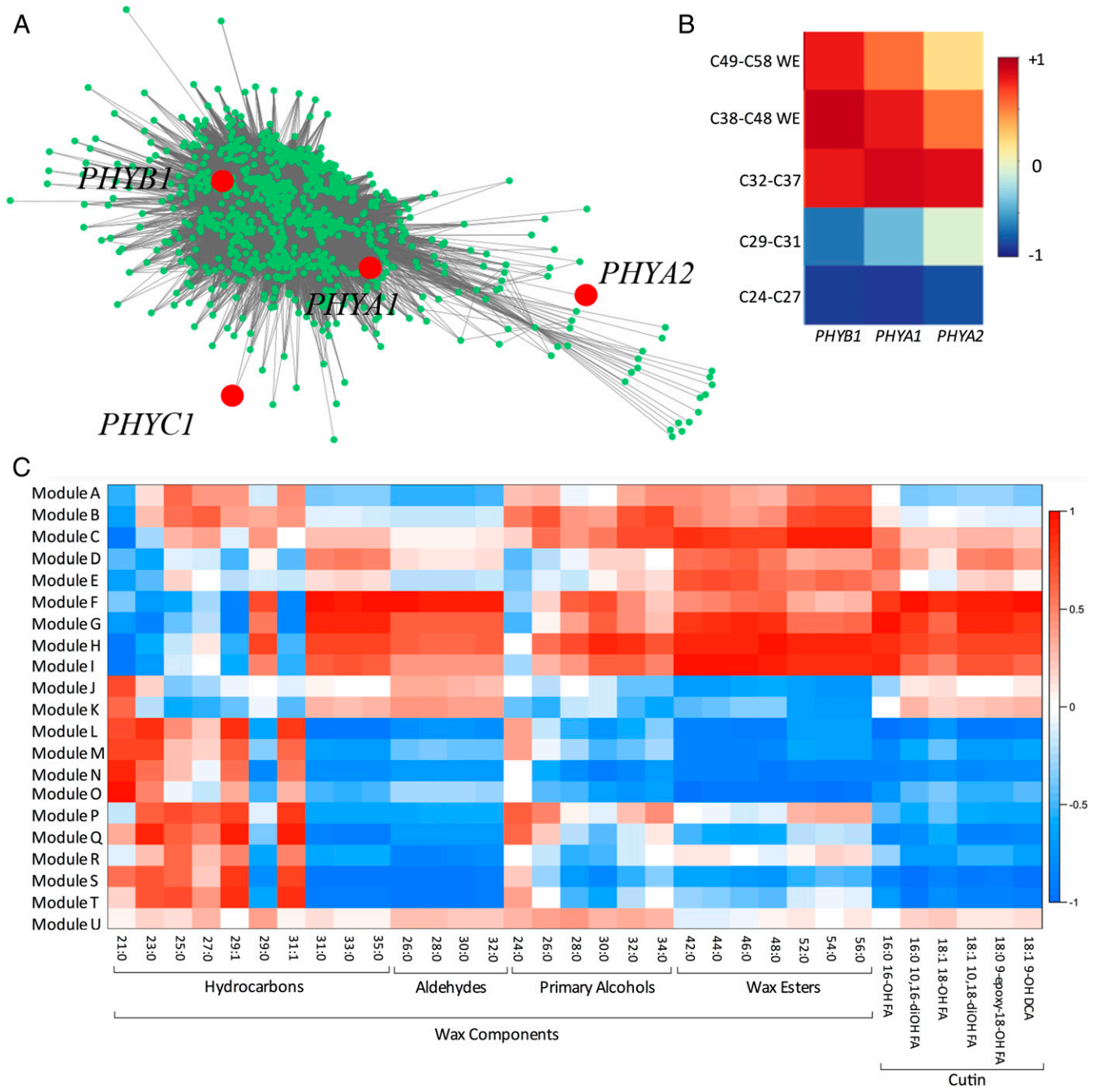

Fig. 3. Coexpression modules correlated with cuticle components of the maize adult leaf. (*A*) Visualization of the coexpression network of module H. The red-colored nodes correspond to the phytochrome homologs *PHYA1*, *PHYA2*, *PHYB1*, and *PHYC1*, some of which (*PHYB1* and *PHYA1*) occupy central positions of the network (with numerous connections with other nodes). (*B*) Correlations between *PHYA1*, *PHYA2*, and *PHYB1* expression and cuticle components—wax esters (WEs) and aliphatics—grouped by chain lengths. (*C*) Heat map depicting the correlation of each cuticle lipid component (*x* axis) to the 21 coexpression modules (*y* axis) identified in transcriptomic analyses of the expanding maize leaf 8. Colors (red to blue) correspond to the values of the Pearson's pairwise correlations, where red (+1) is positively correlated and blue (−1) is negatively correlated. Cuticle lipid abundance data used for this analysis are from Bourgault et al. (25).

mutants as compared with wild-type leaves (Fig. 4*C* and *SI Appendix*, Fig. S4). Although total amounts of alcohols, fatty acids, and alkanes are not significantly altered in *phya1 phya2* double mutants, larger chain-length alcohols (C_{32}, C_{34}, and C_{36}), fatty acids (C_{30}, C_{32}, C_{34}, C_{36}), and alkanes (C_{37}) are overaccumulated in double-mutant cuticles, whereas shorter chain-length alcohols (C_{28}), fatty acids (C_{22} and C_{24}), and alkanes (C_{23}, C_{27}) are underaccumulated as compared with wild-type control leaves (Fig. 4*C*). Analyses of additional *phya1 phya2* double-mutant allele combinations will provide further tests of the model wherein PHYA function regulates cuticle composition in maize leaves, as predicted by our WGCN analysis (Fig. 3*A*).

To determine whether PHY regulation of cuticle accumulation is simply a maize-specific phenomenon or is in fact found in other land plants, equivalent analyses of cuticle lipids were performed on *phy* mutant colonies of the moss *P. patens*, a member of

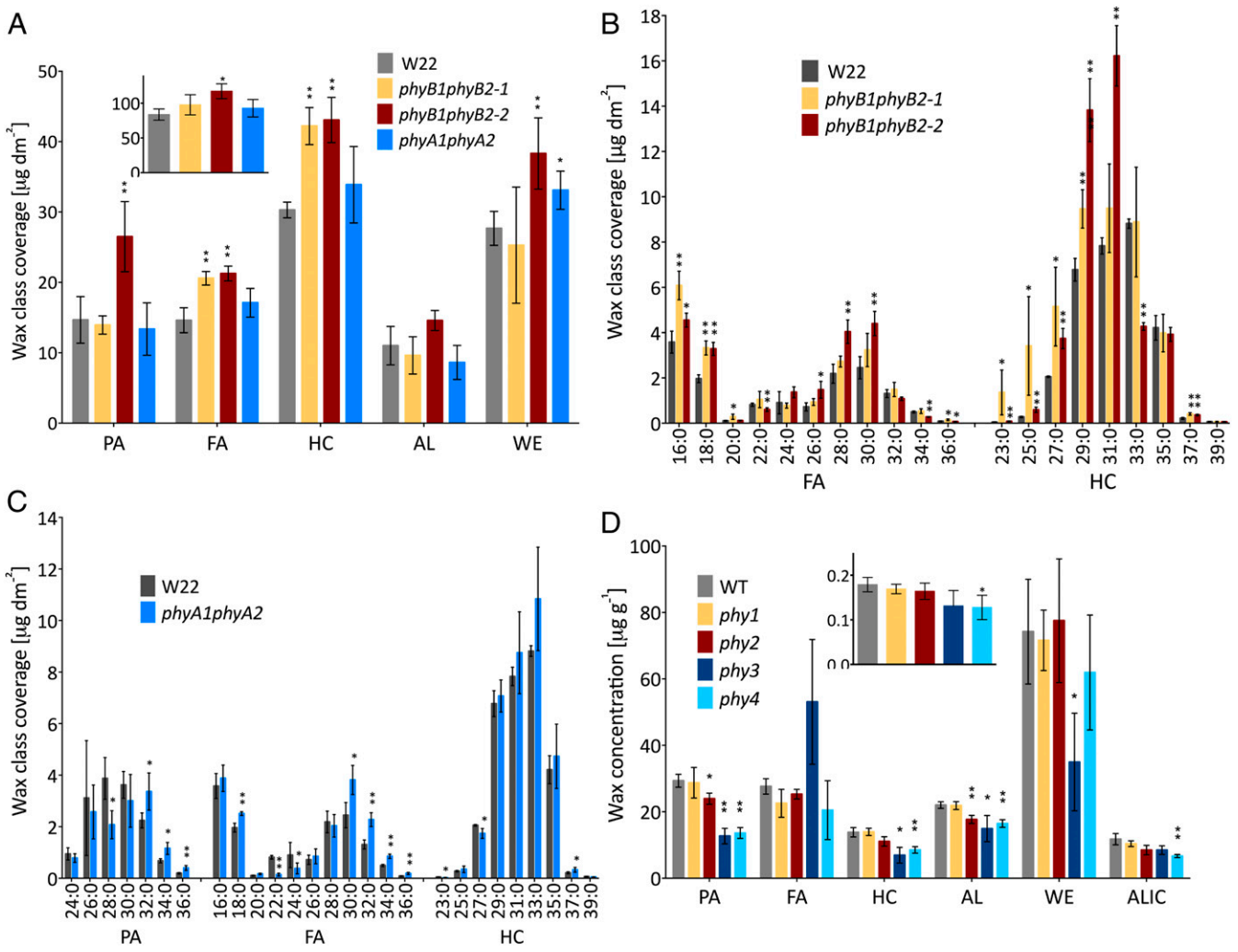

Fig. 4. PHYTOCHROME regulates cuticle wax composition in the adult maize leaf and in the moss *P. patens*. (*A*) Main cuticular wax components in maize *phyB1 phyB2* double mutants and control leaves (W22). (*Inset*) Total wax loads. (*B*) Detailed composition of fatty acids (FAs) and hydrocarbons (HCs) in maize *phyB1 phyB2* double mutants and control waxes. (*C*) Detailed composition of primary alcohols (PAs), FAs, and HCs in maize *phyA1 phyA2* double mutants and control waxes. (*D*) Cuticular wax profiles in gametophyte colonies of *phy* mutants and wild-type *P. patens*. (*Inset*) Total wax loads. Error bars represent SD. Asterisks indicate significant differences with wild type between samples in unpaired *t* tests. AL, aldehyde; WE, wax ester; ALIC, alicyclics. $*P < 0.05$; $**P < 0.01$.

the bryophytes that diverged from later-evolved plant lineages early in the evolution of land plants (9). Physcomitrella contains seven canonical *PHY* genes (*PHY1* to *PHY4* and *PHY5a* to *PHY5c*) (40), all of which lack the N-terminal extension found in angiosperm PHYB (2). Moreover, these ancestral moss *PHY* genes occupy a phylogenetically distinct clade from angiosperm *PHY*s (2), and *PHY* gene duplication and diversification occurred independently in the bryophytes and angiosperms (41). These data imply that the *PHY* genes of Physcomitrella may have unique functions, unlike those described for angiosperm *PHY*s (40–42). Null mutations in four moss *PHY* loci (*phy1* to *-4*) were generated by homologous replacement, as described previously in Mittmann et al. (2). As shown in Fig. 4*D*, analyses of cuticle lipids in moss gametophores revealed that all *P. patens phy* single mutants, except for *phy1*, displayed reductions in several total wax classes as compared with wild-type moss. Specifically, *phy2*, *phy3*, and *phy4* mutants each had significantly reduced amounts of total fatty alcohols and aldehydes, *phy3* and *phy4* were reduced in total alkanes, and *phy3* had reduced wax esters, whereas *phy4* had reductions in alicyclics and total waxes. Moreover, *phy2-4* mutants of moss exhibit some complementary phenotypes. For example, *phy3* cuticles are deficient in longer-chain (carbon number ≥25) aldehydes, whereas *phy4* mutants are depleted in shorter-chain (carbon number ≤26) aldehyde components (*SI Appendix*, Fig. S5). Thus, the cuticle phenotypes of the *phy2-4* mutants in *P. patens* are not equivalent to those of *phyb1 phyb2* or *phya1 phya2* double mutants in maize, perhaps due to diversification of PHY functions after the independent gene duplications of the *PHY* homologs within these embryophyte lineages (41).

Previous studies have shown that expression of several cuticle biosynthesis genes is induced by light (1, 4–7, 31). Intriguingly, light-activated photoenzymes can stimulate the enzymatic conversion of fatty acids to hydrocarbons in green algal relatives of land plants (32, 33), although these lipids are not deposited on algal epidermal surfaces to form a cuticle. Whereas cuticles are an evolutionary innovation of land plants (8–12, 43), PHY light receptors, which regulate a variety of physiological processes during plant growth and development, are found in all green plants including freshwater algae (41, 44). Our data from bryophyte mosses and angiosperm grasses suggest that PHY-mediated light signaling contributes to the regulation of plant cuticle development, as an innovation during the evolution of land plants.

Materials and Methods

Plant Materials. B73 seeds were obtained from the Maize Genetics Cooperation Stock Center; maize plants were grown in 25 °C day, 20 °C night, 60% relative humidity, and 10-h day length Percival A100 growth chambers (Percival Scientific) until harvest.

Solo mutations of maize *phyb1*, comprising three independent *Mutator* (*Mu*) transposon insertion alleles, were analyzed. The *phyb1-563* allele was obtained from P. Dubois, Cascade Specialties, Portland, OR, and R. Sawers, LANGEBIO, Irapuato, Guanajuato, Mexico, and contains a *Mu* insertion in exon 1 within the phytochromobilin chromophore attachment site, and comprises a null allele that makes no detectable PHYB protein (38). Two additional *phyb1* single mutations were identified from Uniform-*Mu* lines (45) obtained from the Maize Genetics Cooperation Stock Center. One allele, UFMU-05410, contains a *Mu* transposon in exon 1, and a second allele, UFMU-03349, also contains a *Mu* transposon insertion in exon 1. Plants were grown in the greenhouse in San Diego, CA.

Two allelic combinations of *phyb1 phyb2*, each introgressed four times into inbred W22, were investigated. The *phyb1 phyb2-1* double-mutant combination was obtained from P. Dubois and R. Sawers and is homozygous for the null mutation *phyb1-563* (described above) and homozygous for *phyb2-12058*, which contains a *Mu* transposon in exon 1 that is located 5′ of the chromophore attachment site (39). The *phyb1*, *phyb2-2* combination was obtained from J. Strable, Cornell University, Ithaca, NY, and is homozygous for the null mutation *phyb1-563* (described above) and homozygous for *phyb2-F2*; the *phyb2-F2* allele contains a large deletion and is a null allele that makes no detectable PHYB protein (38). Plants were grown in the greenhouse in San Diego, CA, as described above.

Five gametophyte stocks of *P. patens*, each containing a solo mutation in *phy1*, *phy2*, *phy3*, or *phy4* (induced by homologous recombination in the Grandsen ecotype) (2), and a wild-type Grandsen control line were obtained from J. Hughes, Justus Liebig University, Giessen, Germany. Plants were grown in growth chambers as described (46).

Laser Microdissection and RNAseq Analysis. The unexpanded eighth leaf of the inbred B73 maize plant was harvested in three biological replicates, three plants per replicate, when the leaf was ∼45 to 55 cm, around 33 d after planting. Leaf 8 was dissected out of the whorl and segmented into 2-cm-long intervals, up to 22 cm from the leaf base, seven of which (six intervals from 2 to 14 cm and one interval from 20 to 22 cm) were fixed and paraplast embedded for use in laser microdissection as described (47). Epidermal and internal tissues were microdissected; RNA was extracted using the PicoPure RNA isolation kit and linearly amplified using the Arcturus RiboAmp HS PLUS RNA Amplification kit. RNAseq libraries were constructed with the NEBNext Ultra RNA Library Prep Kit for Illumina, and the HiSEQ 2500 instrument was used for sequencing. After sequencing, reads were aligned to B73 genome RefGen_v3 with HiSAT2 (48, 49) and counted with HTSeq (50). The raw RNAseq data are available at the National Center for Biotechnology Information Short Reads Archive (NCBI SRA) accession number SRP116320 at the following URL: https://www.ncbi.nlm.nih.gov/Traces/study/?acc=SRP116320&o=acc_s%3Aa.

Wax Extraction and Analysis. Waxes were extracted by submerging the tissue in pure chloroform for 60 s, followed by evaporation under a gentle stream of nitrogen. Dry wax samples were analyzed with gas chromatography–mass spectometry as described previously (25).

Differential Expression Analysis. Differential expression analysis was performed with edgeR 3.3.2 package in R (51, 52). Genes with counts fewer than two counts per million reads were filtered out, and analysis was carried out under False Discovery Rate < 0.1 as the significant measure.

Weighted Coexpression Network Analysis. The correlation between genes was performed using a modified version of Tukey's Biweight correlation (53), which was later used to calculate the distance matrix. The calculations were done using WGCNA 3.3.0 package in R (26). The distance matrix was used for the dynamic hierarchical clustering and to construct the edges (connections) between nodes (genes) in the network. Network analysis of hubs and direct neighbors was done in Python 2.7 using NetworkX 1.11 module (54).

Data Availability. The raw RNAseq data are available at the NCBI SRA accession number SRP116320 at the following URL: https://www.ncbi.nlm.nih.gov/Traces/study/?acc=SRP116320&o=acc_s%3Aa.

All plant materials are available upon request.

ACKNOWLEDGMENTS. The work was funded by NSF Integrative Organismal Systems Award 1444507 and supported in part by funding from the Canada Research Chairs program and the Natural Sciences and Engineering Research Council of Canada (I.M.). We thank all members on the cuticle project for discussion and input, especially M. Vasquez, A. Nguyen, and M. Lin, and S. Leiboff for help in RNAseq processing. We also thank J. Strable, T. Brutnell, R. Sawers, and P. Dubois for the maize *phy* mutant seed; J. Hughes for the *P. patens phy* mutant stocks; M. Vasquez for help in caring for maize *phy* mutant plants; and J. Cammarata for help in growing moss.

1. C. Fankhauser, J. Chory, Light control of plant development. *Annu. Rev. Cell Dev. Biol.* **13**, 203–229 (1997).
2. F. Mittmann *et al*., Targeted knockout in *Physcomitrella* reveals direct actions of phytochrome in the cytoplasm. *Proc. Natl. Acad. Sci. U.S.A.* **101**, 13939–13944 (2004).
3. E. M. Tobin, J. Silverthorne, Light regulation of gene expression in higher plants. *Annual Rev. Plant Physiol.* **36**, 569–593 (1985).
4. M. Chen, J. Chory, C. Fankhauser, Light signal transduction in higher plants. *Annu. Rev. Genet.* **38**, 87–117 (2004).
5. J. Joubès *et al*., The VLCFA elongase gene family in *Arabidopsis thaliana*: Phylogenetic analysis, 3D modelling and expression profiling. *Plant Mol. Biol.* **67**, 547–566 (2008).
6. T. S. Hooker, A. A. Millar, L. Kunst, Significance of the expression of the CER6 condensing enzyme for cuticular wax production in *Arabidopsis*. *Plant Physiol.* **129**, 1568–1580 (2002).
7. M. C. Suh, Y. S. Go, DEWAX-mediated transcriptional repression of cuticular wax biosynthesis in *Arabidopsis thaliana*. *Plant Signal. Behav.* **9**, e29463 (2014).
8. G. Kerstiens, Water transport in plant cuticles: An update. *J. Exp. Bot.* **57**, 2493–2499 (2006).
9. R. M. Bateman *et al*., Early evolution of land plants: Phylogeny, physiology, and ecology of the primary terrestrial radiation. *Annu. Rev. Ecol. Syst.* **29**, 263–292 (1998).
10. R. Jetter, M. Riederer, Localization of the transpiration barrier in the epi- and intracuticular waxes of eight plant species: Water transport resistances are associated with fatty acyl rather than alicyclic components. *Plant Physiol.* **170**, 921–934 (2016).
11. P. Kenrick, P. R. Crane, The origin and early evolution of plants on land. *Nature* **389**, 33–39 (1997).
12. J. A. Raven, D. Edwards, ""Physiological evolution of lower embryophytes: Adaptations to the terrestrial environment"" in *The Evolution of Plant Physiology*, A. R. Hemsley, I. Poole, Eds. (Linnean Society Symposium Series, Elsevier Academic Press, 2004), pp. 17–41.
13. C. E. Jeffree, ""Structure and ontogeny of plant cuticles"" in *Plant Cuticles*, G. Kerstiens, Ed. (Bios Scientific Publishers, 2006), pp. 33–82.
14. M. Pollard, F. Beisson, Y. Li, J. B. Ohlrogge, Building lipid barriers: Biosynthesis of cutin and suberin. *Trends Plant Sci.* **13**, 236–246 (2008).
15. P. E. Kolattukudy, Polyesters in higher plants. *Adv. Biochem. Eng. Biotechnol.* **71**, 1–49 (2001).
16. C. Nawrath, The biopolymers cutin and suberin. *Arabidopsis Book* **1**, e0021 (2013).
17. T. H. Yeats, J. K. Rose, The formation and function of plant cuticles. *Plant Physiol.* **163**, 5–20 (2013).
18. Y. Li-Beisson *et al*., Acyl-lipid metabolism. *Arabidopsis Book* **11**, e0161 (2013).
19. L. Samuels, L. Kunst, R. Jetter, Sealing plant surfaces: Cuticular wax formation by epidermal cells. *Annu. Rev. Plant Biol.* **59**, 683–707 (2008).
20. L. Kunst, L. Samuels, Plant cuticles shine: Advances in wax biosynthesis and export. *Curr. Opin. Plant Biol.* **12**, 721–727 (2009).
21. G. Ingram, C. Nawrath, The roles of the cuticle in plant development: Organ adhesions and beyond. *J. Exp. Bot.* **68**, 5307–5321 (2017).
22. A. L. Girard *et al*., Tomato GDSL1 is required for cutin deposition in the fruit cuticle. *Plant Cell* **24**, 3119–3134 (2012).
23. S. B. Lee, M. C. Suh, Recent advances in cuticular wax biosynthesis and its regulation in Arabidopsis. *Mol. Plant* **6**, 246–249 (2013).
24. P. S. Schnable *et al*., The genetics of cuticular wax biosynthesis. *Maydica* **39**, 279–287 (1994).
25. R. Bourgault *et al*., Constructing functional cuticles: Analysis of relationships between cuticle lipid composition, ultrastructure and water barrier function in developing adult maize leaves. *Ann. Bot.* **125**, 79–91 (2020).
26. P. Langfelder, S. Horvath, WGCNA: An R package for weighted correlation network analysis. *BMC Bioinformatics* **9**, 559 (2008).
27. P. Langfelder, S. Horvath, Fast R functions for robust correlations and hierarchical clustering. *J. Stat. Softw.* **46**, 1–17 (2012).
28. R. Zhong, C. Lee, J. Zhou, R. L. McCarthy, Z. H. Ye, A battery of transcription factors involved in the regulation of secondary cell wall biosynthesis in *Arabidopsis*. *Plant Cell* **20**, 2763–2782 (2008).
29. A. L. Barabási, Network science. *Philos. Trans. Royal Soc. Math. Phys. Eng. Sci.* **371**, 20120375 (2013).
30. A. L. Barabási, Z. N. Oltvai, Network biology: Understanding the cell's functional organization. *Nat. Rev. Genet.* **5**, 101–113 (2004).
31. H. Kim, Y. S. Go, M. C. Suh, DEWAX2 transcription factor negatively regulates cuticular wax biosynthesis in *Arabidopsis* leaves. *Plant Cell Physiol.* **59**, 966–977 (2018).
32. D. Sorigué *et al*., Microalgae synthesize hydrocarbons from long-chain fatty acids via a light-dependent pathway. *Plant Physiol.* **171**, 2393–2405 (2016).
33. D. Sorigué *et al*., An algal photoenzyme converts fatty acids to hydrocarbons. *Science* **357**, 903–907 (2017).

34. M. J. Sheehan, P. R. Farmer, T. P. Brutnell, Structure and expression of maize phytochrome family homeologs. *Genetics* **167**, 1395–1405 (2004).
35. M. Endo, S. Nakamura, T. Araki, N. Mochizuki, A. Nagatani, Phytochrome B in the mesophyll delays flowering by suppressing *FLOWERING LOCUS T* expression in *Arabidopsis* vascular bundles. *Plant Cell* **17**, 1941–1952 (2005).
36. S. A. Casson, A. M. Hetherington, Phytochrome B is required for light-mediated systemic control of stomatal development. *Curr. Biol.* **24**, 1216–1221 (2014).
37. J. Kim *et al*., Epidermal phytochrome B inhibits hypocotyl negative gravitropism non-cell-autonomously. *Plant Cell* **28**, 2770–2785 (2016).
38. M. J. Sheehan, L. M. Kennedy, D. E. Costich, T. P. Brutnell, Subfunctionalization of PhyB1 and PhyB2 in the control of seedling and mature plant traits in maize. *Plant J.* **49**, 338–353 (2007).
39. P. G. Dubois, "Genetic and molecular characterization of maize response to shade signals," PhD thesis, Cornell University, Ithaca, NY (2010).
40. A. L. Ermert, F. Nogué, F. Stahl, T. Gans, J. Hughes, "CRISPR/Cas9-mediated knockout of *Physcomitrella patens* phytochromes" in *Phytochromes*, A. Hiltbrunner, Ed. (Methods in Molecular Biology, Humana, 2019), pp. 3237–3263.
41. F. W. Li *et al*., Phytochrome diversity in green plants and the origin of canonical plant phytochromes. *Nat. Commun.* **6**, 7852 (2015).
42. J. Hughes, G. Brücker, A. Repp, M. Zeidler, F. Mittmann, "Phytochromes and functions: Studies using gene targeting in *Physcomitrella*" in *Light Sensing in Plants*, M. Wada, Y. Shimazo, M. Iino, Eds. (Springer, 2019), pp. 103–110.
43. T. A. Salminen *et al*., Deciphering the evolution and development of the cuticle by studying lipid transfer proteins in mosses and liverworts. *Plants (Basel)* **7**, 6 (2018).
44. D. Duanmu *et al*., Marine algae and land plants share conserved phytochrome signaling systems. *Proc. Natl. Acad. Sci. U.S.A.* **111**, 15827–15832 (2014).
45. D. R. McCarty *et al*., Steady-state transposon mutagenesis in inbred maize. *Plant J.* **44**, 52–61 (2005).
46. C. D. Whitewoods *et al*., CLAVATA was a genetic novelty for the morphological innovation of 3D growth in land plants. *Curr. Biol.* **28**, 2365–2376.e5 (2018).
47. R. Johnston *et al*., Transcriptomic analyses indicate that maize ligule development recapitulates gene expression patterns that occur during lateral organ initiation. *Plant Cell* **26**, 4718–4732 (2014).
48. K. A. G. Kremling *et al*., Dysregulation of expression correlates with rare-allele burden and fitness loss in maize. *Nature* **555**, 520–523 (2018).
49. D. Kim, B. Langmead, S. L. Salzberg, HISAT: A fast spliced aligner with low memory requirements. *Nat. Methods* **12**, 357–360 (2015).
50. S. Anders, P. T. Pyl, W. Huber, HTSeqA Python framework to work with high-throughput sequencing data. *Bioinformatics* **31**, 166–169 (2015).
51. M. D. Robinson, D. J. McCarthy, G. K. Smyth, edgeR: A Bioconductor package for differential expression analysis of digital gene expression data. *Bioinformatics* **26**, 139–140 (2010).
52. D. J. McCarthy, Y. Chen, G. K. Smyth, Differential expression analysis of multifactor RNA-Seq experiments with respect to biological variation. *Nucleic Acids Res.* **40**, 4288–4297 (2012).
53. S. Horvath, *Weighted Network Analysis: Applications in Genomics and Systems Biology*, (Springer, 2011).
54. A. A. Hagberg, D. A. Schult, P. J. Swart, "Exploring network structure, dynamics, and function using NetworkX" in *Proceedings of the 7th Phyton in Science Conference*, G. Varoquaux, J. Millman, Eds. (SciPy, 2008), pp. 11–16.